

Structural rearrangements in the C/W(001) surface system

P. F. Lyman* and D. R. Mullins

Oak Ridge National Laboratory, Oak Ridge, Tennessee 37831-6201

(Received 14 December 1994)

We have investigated the surface structure of the C/W(001) surface system at submonolayer C coverages using Auger-electron spectroscopy and high-resolution core-level photoelectron spectroscopy. Core-level spectroscopy is a sensitive probe of an atom's local electronic environment; by examining the core levels of the W atoms in the selvedge region, we monitored the response of the substrate to C adsorption. The average shift of the 4*f* core-level binding energy provided evidence for a heretofore unknown surface reconstruction that occurs upon submonolayer C adsorption. We also performed line-shape analysis on these core-level spectra, and have thereby elucidated the mechanism by which the low-coverage $(\sqrt{2} \times \sqrt{2})R45^\circ$ structure evolves to a $c(3\sqrt{2} \times \sqrt{2})R45^\circ$ arrangement upon further C adsorption. The line-shape analysis also provides corroborating evidence for a proposed model of the saturated C/W(001)-(5×1) surface structure, and suggests that the first two or three atomic W layers are perturbed by the C adsorption and attendant reconstruction.

I. INTRODUCTION

Although the structures of clean and adsorbate-covered surfaces of tungsten have been extensively studied, little structural work has been reported for the C/W(001) surface system. This is in spite of the fact that C modification can profoundly alter the reactivity of molecules, such as CO,^{1,2} ethane,³ amines⁴ and methanethiol^{5,6} on tungsten surfaces. It is unclear whether this modification in reactivity is related in a simple way to the C atoms (i.e., through simple blocking of active sites) or whether more careful attention needs to be paid to the *structure* of the underlying substrate surface.⁶

Initially, the investigation of the structure of C/W(001) with various coverages of C had been approached, using low-energy electron diffraction (LEED).^{1,7,8} A succession of LEED patterns was observed at submonolayer coverages that could be interpreted as arising from arrangements of C adatoms on an unreconstructed W(001) surface. Specifically, a $(\sqrt{2} \times \sqrt{2})R45^\circ$ pattern was observed at C coverages of <0.5 ML (1 ML = 1.0×10^{15} cm⁻²), and a $c(3\sqrt{2} \times \sqrt{2})R45^\circ$ pattern was seen for coverages near 0.67 ML.⁷ These patterns can be naturally explained by C atoms occupying fourfold hollows in simple patterns [Figs. 1(a) and 1(b)].¹ At saturation, however, a (5×1) pattern was observed which appeared less straightforward to explain. A number of structures have been proposed to account for this LEED pattern.^{1,7-10}

One of the most intriguing results to emerge from these early studies was the relative stability of the W(001) and W(110) surfaces with respect to carburization; although polycrystalline W and the open W(111) face were found to nucleate a bulk carbide phase upon extensive exposure to C, the W(110) and W(001) surfaces did not form bulk carbides upon further C dosing.^{1,7,8} Due to the stability and relatively large unit cell of the observed (5×1) LEED pattern arising from the saturated C/W(001) face, the saturation structure was thought to be composed of a distorted, hexagonal low-index plane of one of the car-

bides of tungsten residing on top of an unreconstructed W(001) substrate.^{1,7-9} Inferences to support this view were later made on the basis of valence-band photoemission⁹ and thermal-desorption spectroscopy.¹ Although

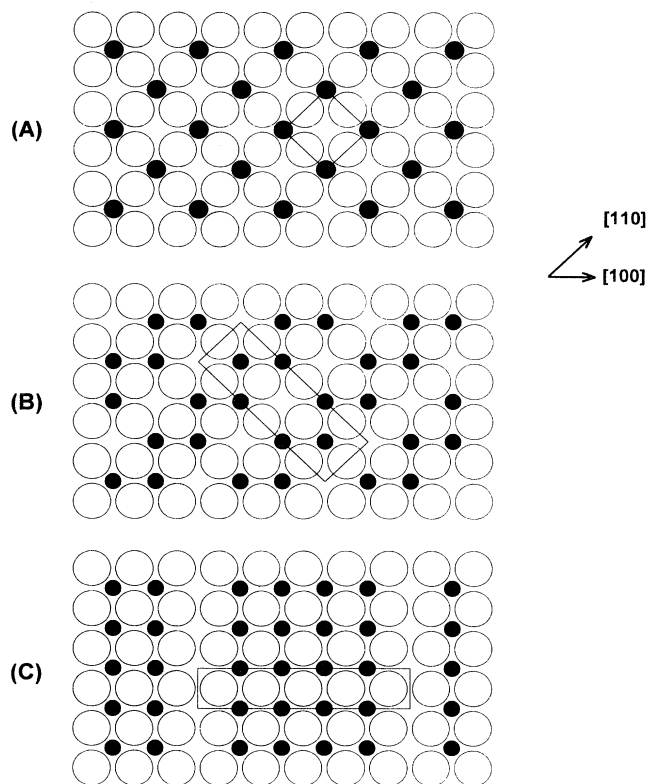


FIG. 1. Schematic representations of various C adlayer structures formed on W(001): (a) $(\sqrt{2} \times \sqrt{2})R45^\circ$, 0.5-ML ideal C coverage; (b) $c(3\sqrt{2} \times \sqrt{2})R45^\circ$, 0.67-ML ideal C coverage; (c) (5×1), 0.8-ML ideal C coverage. Large open circles are first-layer W atoms, and small dark circles are C adatoms.

several variations of the exact scheme emerged, none were able to satisfactorily account for all of the available experimental data.⁹

More recently, however, a study carried out using a local probe, low-energy ion scattering (LEIS), revealed that C atoms on the (5×1) surface occupy essentially the same sites as they do on surfaces of lower coverages, namely, the fourfold hollow of the bcc(001) surface; the underlying substrate was *not* found to undergo any major change in symmetry.¹⁰ Thus, the findings of the LEIS study conflicted with the model for the saturated surface developed in the LEED investigations. An alternative model was proposed, wherein every fifth row of fourfold hollow sites (aligned along a $[100]$ azimuth) is vacant, and the other rows of hollows contain adsorbed C atoms [Fig. 1(c)]. This model then explains the (5×1) periodicity as arising from ordering in the C adatoms, and naturally accounts for the observed saturation coverage of 0.8 ML.

We have investigated this surface as a function of C coverage by undertaking a core-level spectroscopy study to sensitively monitor the local electronic environment of the surface W atoms. The binding energy of the substrate atoms' core electrons is sensitive to adsorbate bonding,^{11–15} reconstruction,¹⁵ and the surface electronic structure.^{16,17} Thus, high-resolution core-level spectroscopy can be used to monitor the response of the *substrate* atoms to adsorbates, and can provide insight to the local environment that is complementary to the long-range-order information that LEED provides. Using this technique, we have found strong evidence for a previously unknown surface reconstruction that occurs upon submonolayer C adsorption. We have elucidated the mechanism by which the $(\sqrt{2} \times \sqrt{2})R45^\circ$ structure evolves to $c(3\sqrt{2} \times \sqrt{2})R45^\circ$ arrangement. Finally, we have provided corroborating evidence for the veracity of the simple (5×1) structure proposed in the LEIS (Ref. 10) study.

II. EXPERIMENT

The measurements were made in a cryogenically pumped stainless steel vacuum chamber having a base pressure of less than 1×10^{-10} torr. The system was attached to beamline U12B (Ref. 18) of the National Synchrotron Light Source (NSLS) at Brookhaven National Laboratory to provide monochromatic photons of 20–120 eV. Using Laue back reflection, the W(001) single crystal was mechanically polished and aligned to within 0.5° of the (001) direction. The sample was mounted on W wires and could be cooled by liquid nitrogen to 100 K and heated resistively to 1500 K or by electron bombardment to > 2200 K. A W/5% Re vs W/26% Re thermocouple was used to monitor the temperature. Cleaning was accomplished by repeatedly flashing the sample to 2300 K in an oxygen ambient (which effectively removed C and other contaminants), followed by a final flash in ultrahigh vacuum to 2300 K to desorb the remaining O. Sample cleanliness was monitored by Auger-electron spectroscopy (AES), using a Perkin Elmer single pass cylindrical mirror analyzer. Desired C coverages were achieved by exposing the substrate to ethylene

through a gas dosing tube.¹³ The substrate was held at 400 K during the exposure, and subsequently annealed to 1000 K to desorb any residual H and to increase the surface order. The *saturated* surface was prepared by exposing the substrate to ethylene at a substrate temperature of 1500 K. C coverages were determined by AES using the ratio of the C peak at 272 eV to the W peak at 350 eV. The saturation coverages when dosing at 400 and 1500 K were assumed to be 0.67 and 0.80 ML, respectively.¹⁰ Photoemission spectra of the W $4f$ region were then recorded using 70-eV photons and a VSW CLASS 100 hemispherical analyzer. Total instrumental energy resolution was ≈ 150 meV; binding energies were referenced to the Fermi level. Each C coverage was prepared independently, starting from a clean W substrate. Core-level and Fermi-level photoemission spectra were recorded from each clean and C-covered surface to minimize systematic errors.

III. RESULTS

A. Qualitative appearance of spectra

Representative W $4f_{7/2}$ core-level spectra for several C coverages are shown in Fig. 2. The clean surface contains three features having distinguishable binding energies. The bulk peak *B* has been reported to have a binding energy of 31.44 ± 0.05 eV.^{11,13–16} Due to the reduced coordination of the surface and second atomic layers,¹⁶ the binding energies of those layers' core levels are shifted toward the Fermi level; the surface feature is denoted S_1

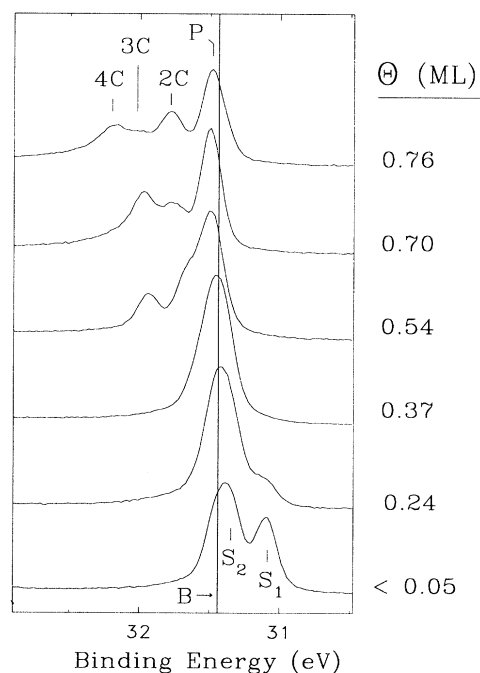


FIG. 2. Representative photoelectron spectra from the W $4f_{7/2}$ core-level region at various C coverages. Clean surface, bulk, and C-induced surface features are indicated. Note the shift of the peak at bulk position.

and it has a surface core-level shift (CLS) of -350 meV with respect to the bulk peak, while the feature arising from the second atomic layer is denoted S_2 and has a shift of -150 meV.¹⁴ The small CLS of the second atomic layer results in a single broadened peak near the bulk binding energy (bottom spectrum in Fig. 2). These surface-related features are modified by the addition of C, eventually resulting in the introduction of at least three features with binding energies deeper than the bulk peak (top spectra in Fig. 2). We denote these features as $2C$, $3C$, and $4C$, in order of shallowest to deepest binding energy.

The simplest analysis of these spectra considers the shift in the centroid, $\bar{E} = \int I(E)E dE / \int I(E) dE$, of the $W 4f_{7/2}$ region as a function of C coverage. The average energy shift, $\Delta\bar{E}$, is defined as the difference between the $W 4f_{7/2}$ centroid from the C covered and clean surfaces. $\Delta\bar{E}$ as a function of C coverage is plotted in Fig. 3. The coverage ranges over which characteristic LEED patterns have been observed in previous work^{1,7,8,10} are indicated schematically at the top of the figure. The solid curve is a least-squares fit to the data of three piecewise-continuous straight line segments. It is evident that below about 0.4 ML, there is a linear change in $\Delta\bar{E}$ with C coverage, followed by a sudden increase in slope at about 0.45 ML. The slope decreases dramatically at about 0.6 ML.

B. Line-shape analysis

A more detailed analysis was also performed by fitting the spectra to a series of peaks at different binding energies using a nonlinear, least-squares fitting program. We employed the asymmetric Doniach-Sunjic line shape¹⁹ for

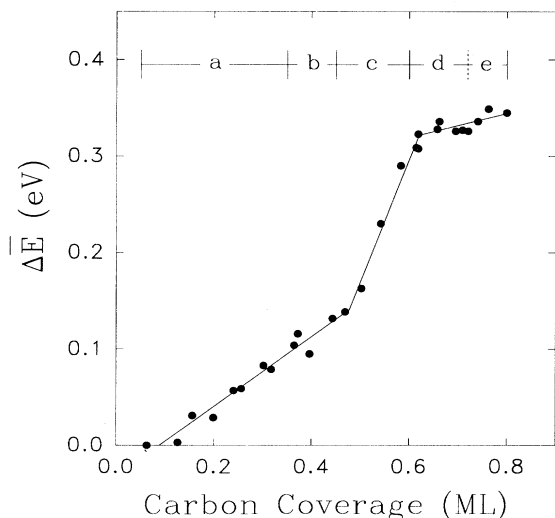


FIG. 3. Difference of centroids of spectra from clean and C-covered surfaces as a function of C coverage. The LEED patterns arising over different coverage regions are indicated: (a) (1×1) , (b) $(\sqrt{2} \times \sqrt{2})R45^\circ$, (c) $(n\sqrt{2} \times \sqrt{2})R45^\circ$ [superstructure spots are extended into lobes along (11) -like directions], (d) $(3\sqrt{2} \times \sqrt{2})R45^\circ$, (e) (5×1) .

all peaks, and allowed a linear background to be varied during the fit; these line shapes were convolved with a Gaussian response function to account for the finite instrumental resolution. Figure 4 depicts the results of the fitting procedure for the spectra shown in Fig. 2. Following the work of Riffe, Wertheim, and Citrin,¹⁵ a strict procedure was employed in order to decompose unresolved features with the greatest accuracy and reliability. For a given C coverage, we first fit the $W 4f_{7/2}$ spectrum from the corresponding clean surface. Peaks arising from the bulk, and clean surface and second layer atoms were then held fixed at the same energy, while fitting the spectrum from the C-covered surface, allowing only their intensities to vary. Additional components were introduced to account for other features remaining in the spectra. We assumed several physically reasonable constraints in order to minimize the number of free parameters in the fit: peaks arising from the second and deeper layers were constrained to have a common asymmetry and lifetime width, while all resolvable features originating from the surface were likewise constrained to have a common asymmetry and lifetime. Excellent fits were obtained, using this procedure for all coverages. At coverages > 0.5 ML, the separation of the C-induced

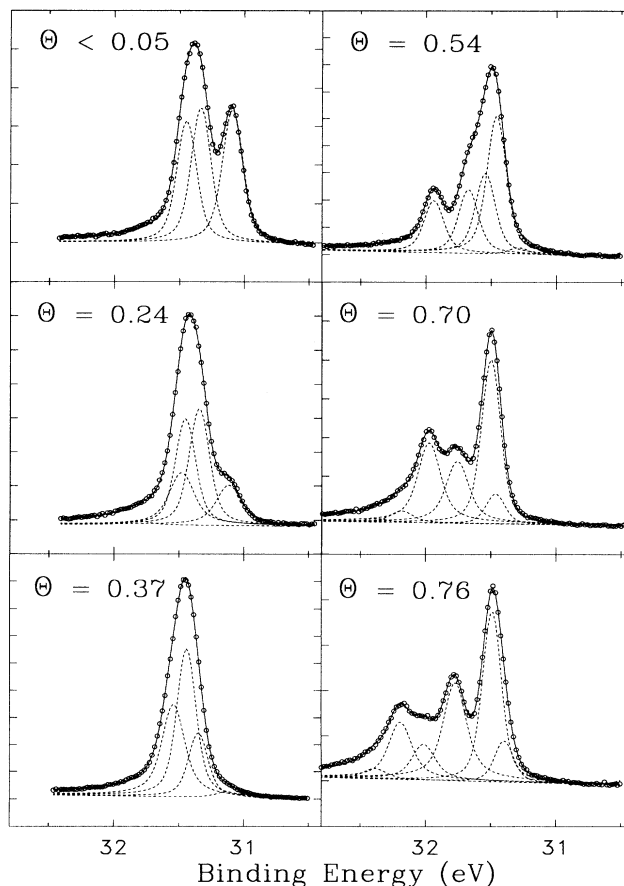


FIG. 4. Representative $W 4f_{7/2}$ spectra and fitted Doniach-Sunjic components. Solid line is overall fit, and dashed lines represent individual fitted features.

features was greater than the experimental resolution and intrinsic widths, facilitating decomposition. However, for the coverages below about 0.5 ML, the C-induced features could not be reliably separated from the bulk peak. Hence, we have chosen to consider the intensity of the composite peak for these coverages, as discussed below.

The fractional intensities of the components found on the clean surface, B , S_1 , and S_2 , are shown as a function of C coverage in Fig. 5(a), while the intensities of the C-induced features $2C$, $3C$, and $4C$ are plotted in Fig. 5(b). The curves through the data are intensities predicted by our model of the evolution of the surface, as discussed below. The CLS (with respect to the bulk binding ener-

gy) of all the features is plotted as a function of C coverage in Fig. 6.

IV. DISCUSSION

A. $(\sqrt{2} \times \sqrt{2})R45^\circ$

(i) *Average core-level shifts.* It was unequivocally demonstrated in the earlier LEIS study¹⁰ that the C atoms occupied fourfold hollow sites throughout the entire coverage range. As C is deposited, each C adatom increases the W-C coordination of four surface W atoms. The linear increase in $\Delta\bar{E}$ (Fig. 3) between 0 and 0.45 ML can be attributed solely to the increased W-C coordination as the $(\sqrt{2} \times \sqrt{2})R45^\circ$ structure is formed. No changes in the W surface structure or in the W-C bonding are indicated in this coverage range.

(ii) *Line-shape analysis.* The S_1 component is linearly attenuated upon addition of C [Fig. 5(a)]. The presence of a C atom in a fourfold hollow site is evidently sufficient to alter the binding energy of the surrounding W atoms, so that they no longer contribute to the S_1 peak. A $(\sqrt{2} \times \sqrt{2})R45^\circ$ LEED pattern emerges at coverages as low as 0.35 ML.¹⁰ The appearance of a $(\sqrt{2} \times \sqrt{2})R45^\circ$ pattern below 0.5 ML indicates that the adatoms must cluster into islands having the ideal $(\sqrt{2} \times \sqrt{2})R45^\circ$ structure. The rate at which the S_1 peak is attenuated can reveal how large the islands grow for these deposition conditions. For example, if the C islands were extremely small (or if the adatom-adatom interaction happened to be repulsive), the S_1 component would be eliminated by about 0.25 ML. If, on the other hand, the C islands were very large, the S_1 component would not be completely extinguished until about 0.5 ML. Although there is undoubtedly a distribution of island sizes in the real system, we have calculated the expected rate of extinction of the S_1 component for different sizes of C islands, assuming that all C islands have the same size. The dashed line in Fig. 5(a) through the S_1 data is the expected extinction rate if all C islands contained 12 C atoms, and it provides a reasonable fit to the data.

The disappearance of S_1 as a function of C coverage can be contrasted with what happens when S is adsorbed on W(001).¹³ As the S coverage is increased, the S_1 peak is extinguished by 0.25 ML. A peak appears midway between S_1 and B . This peak has a maximum intensity at 0.25 ML and disappears by 0.5 ML. These observations are all consistent with the adsorption of S adatoms in fourfold sites in a $p(2 \times 2)$ structure at coverages up to 0.25 ML. In the $p(2 \times 2)$ structure, each surface W atom is coordinated to one adatom compared to two adatoms in the $(\sqrt{2} \times \sqrt{2})R45^\circ$ structure; thus, only 0.25 ML S atoms arranged in a $p(2 \times 2)$ pattern are sufficient to affect each surface W atom.

The S_2 component is also attenuated by the addition of C. The bcc(001) surface is relatively open, so that a C atom in a fourfold hollow can bond directly to the second-layer atom. The distance from the top-layer C site to the second-layer W position is 2.08 Å, whereas the distance from the C site to the first-layer W position is 2.28 Å.¹⁰ Therefore, second-layer W atoms would be

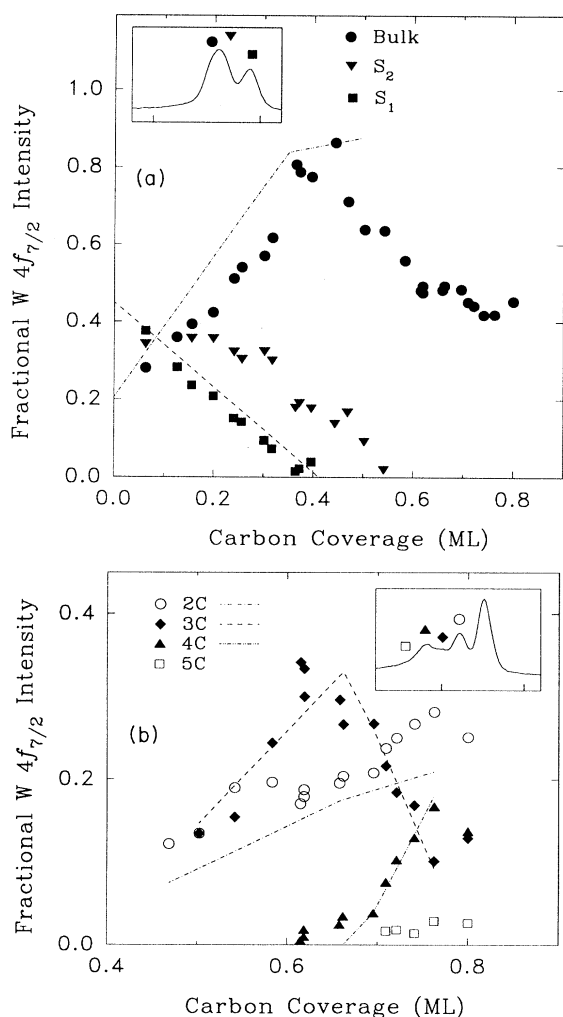


FIG. 5. (a) Fractional intensity of clean surface features (B , S_2 , and S_1) as a function of C coverage. Lines are fits to models discussed in the text. Inset depicts the position of the plotted features on clean surface spectrum. (b) Fractional intensity of C-induced surface features ($2C$, $3C$, $4C$, and $5C$) as a function of C coverage. The lines represent fits to model described in the text. Inset depicts position of the plotted features on high-coverage surface spectrum.

readily affected by C adatoms; thus, it is not surprising that the S_2 component is affected by C. There does not, however, appear to be a 1:1 or even a linear relationship between C coverage and S_2 intensity. The changes in S_2 may reflect some structural change, such as a change in the first-to-second layer relaxation.

Below about 0.45 ML, surface- and second-layer W atoms that are modified by C evidently acquire a $4f$ binding energy close to that of bulk W. Thus, the intensity lost from the S_1 and S_2 components contributes to a broad peak near the bulk peak position. Although this composite peak surely contains multiple components, the experimental resolution and/or the intrinsic separation was not great enough to allow us to reliably decompose these components. Thus the "bulk" peak intensity plotted in Fig. 5(a) grows nearly linearly with increasing C coverage up to about 0.4 ML, and includes contributions from bulk and C-modified surface atoms. The dot-dashed line through the bulk peak data was calculated as the sum of initial bulk peak intensity, plus a fraction of the initial S_1 and S_2 intensities proportional to C coverage, computed by assuming that every deposited C atom causes the neighboring surface and second-layer W atoms to acquire a bulklike binding energy. Above 0.45 ML the composite B peak intensity decreases as the contribution from the surface atoms shifts to resolvable peaks at higher-binding energy.

B. Transition from $(\sqrt{2} \times \sqrt{2})R45^\circ$ to $c(3\sqrt{2} \times \sqrt{2})R45^\circ$

(i) *Average core-level shifts.* Figure 2 shows that the change in $\Delta\bar{E}$ per added C atom (i.e., slope) is constant only up to about 0.45 ML, and then attains a much greater value up to about 0.6 ML. Since increased W-C coordination alone cannot account for this change, it appears that the average W-W coordination of the near-surface layers is changing in the coverage range of 0.45–0.6 ML. This implies that the W surface layer or layers are undergoing a reconstruction in this range. Changes in the slopes of $\Delta\bar{E}$ vs coverage were also seen in the H/W(110) (Ref. 15) and N/W(001) systems,¹¹ due to the reconstruction of those systems' surfaces. Furthermore, the LEIS study¹⁰ observed some evidence for a lateral shift of the surface W layer (0.3 Å) at high C coverages.

Another possibility is that the bonding interaction between the C and the W is changing, thus altering the chemical shift of the core levels. For example, if the system was becoming more "carbide-like," i.e., greater electron charge on the C, the W core levels would be expected to shift to greater binding energy as is observed. However, C 1s spectra taken at low and high carbon coverages (not shown) demonstrate that the C 1s core level does not shift, thus indicating that the C-W bonding interaction is not changing.

(ii) *Long-range order.* In the $(\sqrt{2} \times \sqrt{2})R45^\circ$ structure, alternate rows of fourfold hollow sites, aligned along the [110] azimuth, are occupied by C atoms, while the intervening hollow sites are vacant [Fig. 1(a)]. Two adjacent domains with a $(\sqrt{2} \times \sqrt{2})R45^\circ$ structure may be in phase or may be separated by an antiphase domain

boundary. A domain boundary may have two adjacent vacant rows of hollow sites (a *light* domain wall) or two adjacent occupied rows (a *heavy* domain wall).

In the C/W(001) system, the superstructure LEED spots of the $(\sqrt{2} \times \sqrt{2})R45^\circ$ pattern begin to blur and extend into lobes along the (11)-like directions, as the C coverage increases above 0.45 ML.⁷ The lobes extend with greater coverage and then coalesce into third-order spots, forming the $c(3\sqrt{2} \times \sqrt{2})R45^\circ$ pattern at about 0.6 ML. The ideal $c(3\sqrt{2} \times \sqrt{2})R45^\circ$ structure has C coverage of 0.67 ML, and is formed by repeating the pattern of two adjoining [110] rows of fourfold hollow sites occupied by C, followed by one vacant row [Fig. 1(b)]. Locally, this is similar to a heavy domain wall between $(\sqrt{2} \times \sqrt{2})R45^\circ$ patches. The system of S/W(001) undergoes a similar evolution in LEED pattern.^{20,21} The extension of the half-order spots into lobes in this system has been shown to be consistent with an introduction of heavy domain walls with a statistical distribution of defects.²² The picture of the transition that emerges from the LEED work, therefore, is an accommodation of additional C above the ideal 0.5-ML $(\sqrt{2} \times \sqrt{2})R45^\circ$ structure by addition of heavy domain walls. The density of these walls increases until they neighbor one another to form the ideal 0.67-ML $c(3\sqrt{2} \times \sqrt{2})R45^\circ$ structure.

(iii) *Line shape analysis.* At 0.45 ML all of the W $4f$ intensity has shifted into the composite peak near the bulk peak position. Above that coverage, the intensity from atoms in the surface region that had been indistinguishable from the bulk at low coverages, shifts to form resolvable features at deeper binding energies, thus resulting in the loss in intensity of B at higher coverage [Fig. 5(a)]. Three additional features appear at deeper binding energies than the bulk peak. We attribute these features to surface W atoms in reconstructed regions that are coordinated to two, three, or four C atoms; thus, we denote these as the 2C, 3C, and 4C peaks. We will argue based on the binding energy and behavior of the intensity of these features that the shallowest one is 2C, the middle one is 3C, and the deepest one is 4C. There is also evidence for a small 5C feature at the highest coverages. The binding energy difference between these features is nearly constant, with an average value of 215 meV (Fig. 6).

In an ideal $(\sqrt{2} \times \sqrt{2})R45^\circ$ structure, every surface W atom is coordinated to two C atoms. The addition of one C atom to this structure results in the conversion of four W atoms having two C neighbors into four W atoms with three C neighbors. This accounts for the rapid growth of the 3C feature above 0.45 ML [Fig. 5(b)].

The behavior of the observed 2C feature is more difficult to analyze. Since, in an ideal $(\sqrt{2} \times \sqrt{2})R45^\circ$ structure, every surface W atom *already has* two C neighbors, one might expect that a 2C feature would be present even at low coverages. However, we argued above that it was the additional W-W coordination induced by a reconstruction that shifted the core-level binding energies to deeper than the bulk value (and, therefore, resolvable from the bulk peak). We expect, therefore, that only W atoms with two C neighbors *and* in a reconstructed region will contribute to the 2C feature. The spectra con-

tain a feature that starts as a part of the composite “bulk” peak at about 0.45 ML that shifts continuously to deeper binding energies (and grows in intensity) with greater C coverage. This feature and its shift are easily discernible in the raw spectra (see the 0.54- and 0.70-ML spectra in Fig. 2). Figure 6, which plots the CLS of each feature as a function of C coverage, reveals this behavior more quantitatively; the CLS of the 2C feature is seen to shift linearly with coverage from 160 meV at 0.45 ML to 300 meV at 0.67 ML. The fact that the binding energy of the 2C feature, and not merely its intensity, depends on coverage indicates that the reconstruction is not a strictly local effect. Instead, the increase in W-W coordination in a given reconstructed region must depend on the fraction of the surface that has undergone reconstruction. Perhaps the “extra” C in a heavy domain wall induces a stress on the surrounding material. If the domain wall is isolated, this stress may be accommodated over a relatively large area, causing only a small increase in average W-W coordination. If the density of heavy domain walls is high, however, the stress from nearby domain walls accumulates and must be relieved by larger local distortions, causing a larger increase in average W-W coordination. [A similar coverage-dependent shift was observed in the H/W(110) surface system.¹⁵] The fact that the observed intensity of the 2C feature is increasing over this coverage range, when the absolute number of W atoms with two C neighbors is decreasing, supports our supposition that only W atoms with two C neighbors *and* in reconstructed domains contribute to the 2C feature.

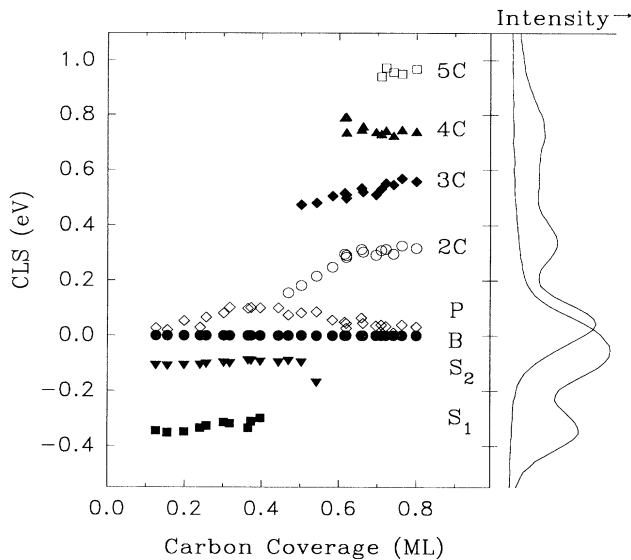


FIG. 6. Surface core-level shifts (referenced to the bulk) of clean and C-induced features as a function of C coverage. Spectra (from clean surface and high-coverage surface) at right axis of figure demonstrate features corresponding to data points. Note that at low coverages, the component denoted as P (“perturbed”) represents the intensity from C-modified *surface* atoms (whose binding energy is nearly degenerate with the bulk peak), while at high coverages, P represents *subsurface* atoms, whose environment has been modified by the reconstructed C/W top layers.

C. Transition from $c(3\sqrt{2}\times\sqrt{2})R45^\circ$ to (5×1)

(i) *Average core-level shifts.* As discussed above, the change in $\Delta\bar{E}$ per added C atom (i.e., the slope in Fig. 2) changes abruptly at about 0.45 and 0.6 ML. We argued above that the dramatic increase in slope at 0.45 ML revealed the onset of a reconstruction in the surface layer that increased the average W-W coordination. Similarly, the reduction of the slope at 0.6 ML provides evidence that the average W-W coordination is no longer increasing above 0.6 ML. The fact that the slope has a smaller value above 0.6 ML than it did in the 0–0.4-ML region may even indicate that the average W-W coordination is decreasing somewhat, since the C atoms continue to populate the same site even at high coverages,¹⁰ thereby making the change in average C-W coordination per added C atom the same for all coverages. However, the value of the slopes in the low- and high-coverage regimes are comparable, making it impossible to conclude this last point with any certainty. We conclude that the reconstruction occurring between 0.45 and 0.6 ML is completed by about 0.6 ML.

(ii) *Long-range order.* In contrast to the transition from $(\sqrt{2}\times\sqrt{2})R45^\circ$ to $c(3\sqrt{2}\times\sqrt{2})R45^\circ$, the transition to the (5×1) structure is not continuous. Instead, the LEED patterns at coverages above about 0.6 ML, but below the saturation coverage of 0.8 ML exhibit a superposition of $c(3\sqrt{2}\times\sqrt{2})R45^\circ$ and (5×1) patterns.¹⁰ This indicates that domains of the (5×1) structure are nucleated and grow at the expense of the lower coverage $c(3\sqrt{2}\times\sqrt{2})R45^\circ$ phase. Hence, additional C is accommodated in this transition through the growth of the more C-rich (5×1) domains.

(iii) *Line-shape analysis.* In an ideal $c(3\sqrt{2}\times\sqrt{2})R45^\circ$ structure, $\frac{1}{3}$ of the surface W atoms have two C neighbors, $\frac{2}{3}$ have three C neighbors, and none have four C neighbors. In the ideal (5×1) structure proposed by Mullins and Overbury,¹⁰ however, 0.4 of the surface W atoms have two C neighbors, 0.6 have four C neighbors, and *none* of the surface W atoms have exactly three C neighbors. Therefore, as (5×1) domains grow at the expense of $c(3\sqrt{2}\times\sqrt{2})R45^\circ$ domains, we expect (1) the intensity of the 2C feature to increase slightly, (2) the intensity of the 3C feature to decrease rapidly, and (3) the intensity of the 4C feature to increase dramatically. This is indeed what we observe [Fig. 5(b)].

We constructed a simple model to describe this behavior more quantitatively. The model assumes that all of the surface is covered with patches having either clean surface, $(\sqrt{2}\times\sqrt{2})R45^\circ$, $c(3\sqrt{2}\times\sqrt{2})R45^\circ$, or (5×1) structure. We assume that there are three critical coverages; the lowest one corresponds to the onset of the $c(3\sqrt{2}\times\sqrt{2})R45^\circ$ reconstruction (≈ 0.45 ML), the second one corresponds to the introduction of (5×1) patches (≈ 0.6 ML), and the final one is just the saturation coverage (0.8 ML), where we assume the entire surface has the (5×1) structure. For any C coverage Θ_C , it is straightforward to calculate the fraction of the surface that must be covered by a particular structure in order to account for all of the surface C. We assume that each surface atom in a reconstructed region makes an equal

contribution to one of the observed (2C, 3C, or 4C) peaks. The data were fit by simultaneously fitting the observed 2C, 3C, and 4C intensities as a function of Θ_C to the calculated number of W atoms bonded to two, three, or four C atoms (based on the fraction of W atoms having two, three, or four C neighbors in each of the ideal, reconstructed structures). The only free parameters, then, were the lower two critical coverages, and an overall normalization factor. The results are shown as the dashed lines in Fig. 5(b); they give a reasonable description of the data. Note that the intensity of the 2C feature is greater than what is predicted by the model and is greater than the intensity of the 4C feature even at high coverages. This may mean that our assumption that the intensity of a given feature per contributing surface W atom is the same for all features (i.e., our use of one overall normalization factor) is not valid. The general trends, however, are well reproduced by the model.

D. Substrate response

On the clean surface, there are only three distinguishable components, which have been assigned to the bulk, first atomic layer, and second atomic layer. Thus, the bulk peak incorporates the intensity from all atoms in the third and deeper layers ($3 \rightarrow \infty$). At high carbon coverages, there are four distinguishable peaks; all but the bulk peak have been assigned to atoms in the first atomic layer. In this case, the "bulk" peak should incorporate intensity from all atoms in the second and deeper layers ($2 \rightarrow \infty$). For the high C coverages, the "bulk" peak exhibited a small (50 meV), but consistent shift to deeper binding energies compared to the bulk peaks on the clean spectra, and also showed some intensity remaining at the clean surface position. (See Fig. 2.) Thus, the "bulk" peak for the high C coverages is actually a composite peak. Presumably, the component that remains at the clean surface binding energy corresponds to the true bulk position, while the shifted component comes from atomic layers in the selvedge (near surface) region that are perturbed by the C adsorption and/or attendant W reconstruction. It has been shown that C can be adsorbed into the selvedge region.²³ By holding one peak fixed at the clean surface bulk position during fitting, we were able to separate the components, as indicated by *P* and *B* in Fig. 6.

Although it is tempting to try to interpret the relative magnitudes of these components to try to ascertain how many atomic layers in the selvedge region are affected by the C/W surface layer, the phenomenon of photoelectron

diffraction presents serious difficulties for such a treatment. For W(110), it has been established that final-state effects can cause significant variations of photoelectron intensity with emission angle and energy.^{24,25} Furthermore, significant variation of the observed surface-to-bulk ratio for the clean surface of W(001) has been reported in previous publications.^{11,13,14,16} Therefore, we will only note that, ignoring possible photoelectron-diffraction effects, the measured relative intensities are in qualitative agreement with a shift in the binding energies occurring in the second and possibly the third W layers, due to the effect of the C/W reconstructed overlayer.

V. CONCLUSIONS

In this study, we have used high-resolution core-level photoelectron spectroscopy to investigate the surface structure and substrate response of the C/W(001) surface system at submonolayer C coverages. We have uncovered strong evidence for a reconstruction of the W(001) surface that is completed at a C coverage of about 0.6 ML. Line-shape analysis of the core-level spectra has allowed us to follow the evolution of the surface, from the low-coverage $(\sqrt{2} \times \sqrt{2})R45^\circ$ structure to the intermediate $c(3\sqrt{2} \times \sqrt{2})R45^\circ$ arrangement, to the (5×1) saturation structure. The mechanisms of these two transitions differ: the first transition occurs continuously, whereas the final transition occurs by nucleation and growth of the high-coverage structure. This analysis has provided corroborating evidence for the proposed model¹⁰ of the saturated C/W(001)- (5×1) surface structure. Finally, it is suggested that the first two or three atomic W layers may be perturbed by the C adsorption and attendant reconstruction.

ACKNOWLEDGMENTS

The authors thank S. H. Overbury and D. M. Zehner for helpful and clarifying discussions. Research sponsored by the Division of Material Sciences (PFL) and the Division of Chemical Sciences (DRM), Office of Basic Energy Sciences, U.S. Department of Energy under Contract No. DE-AC05-84OR21400 with Martin Marietta Energy Systems, Inc. and in part through a grant from the U.S. Department of Energy administered by Oak Ridge Associated Universities. The National Synchrotron Light Source at Brookhaven National Laboratory is supported by the Division of Chemical Sciences and Division of Material Sciences of the U.S. Department of Energy under Contract No. DE-AC02-76CH00016.

*Present address: Brookhaven National Laboratory, National Synchrotron Light Source, Building 725A/X15A, Upton, NY 11973.

¹J. B. Benziger, E. I. Ko, and R. J. Madix, *J. Catal.* **54**, 414 (1978).

²C. M. Friend, J. G. Serafin, E. K. Baldwin, P. A. Stevens, and R. J. Madix, *J. Chem. Phys.* **887**, 1847 (1987).

³A. C. Liu and C. M. Friend, *J. Chem. Phys.* **87**, 4975 (1987).

⁴K. A. Pearlstine and C. M. Friend, *J. Am. Chem. Soc.* **108**, 5837 (1986).

⁵J. B. Benziger and R. E. Preston, *J. Phys. Chem.* **89**, 5002 (1985).

⁶D. R. Mullins and P. F. Lyman, *Prepr. Division Petroleum Chem.* **38**, 688 (1993).

- ⁷D. F. Ollis and M. Boudart, *Surf. Sci.* **23**, 320 (1970).
- ⁸K. J. Rawlings, S. D. Foulas, and B. J. Hopkins, *J. Phys. C* **14**, 5411 (1981).
- ⁹P. M. Stefan, M. L. Shek, and W. E. Spicer, *Surf. Sci.* **149**, 423 (1985).
- ¹⁰D. R. Mullins and S. H. Overbury, *Surf. Sci.* **193**, 455 (1988).
- ¹¹J. Jupille, K. G. Purcell, and D. A. King, *Solid State Commun.* **58**, 529 (1986).
- ¹²F. J. Himpsel, J. F. Morar, F. F. McFeely, R. A. Pollak, and G. Hollinger, *Phys. Rev. B* **30**, 7236 (1984).
- ¹³D. R. Mullins, P. F. Lyman, and S. H. Overbury, *Surf. Sci. Lett.* **285**, L473 (1993).
- ¹⁴J. F. van der Veen, F. J. Himpsel, and D. E. Eastman, *Solid State Commun.* **40**, 57 (1981).
- ¹⁵D. M. Riffe, G. K. Wertheim, and P. H. Citrin, *Phys. Rev. Lett.* **65**, 219 (1990).
- ¹⁶D. Spanjaard, C. Guillot, M.-C. Desjonqueres, G. Treglia, and J. Lecante, *Surf. Sci. Rep.* **5**, 1 (1985).
- ¹⁷P. H. Citrin and G. K. Wertheim, *Phys. Rev. B* **27**, 3176 (1983).
- ¹⁸B. P. Tonner, *Nucl. Instrum. Methods* **172**, 133 (1980).
- ¹⁹S. Doniach and M. Sunjic, *J. Phys. C* **3**, 285 (1970).
- ²⁰A. K. Bhattacharya, L. J. Clarke, and L. M. de la Garza, *J. Chem. Soc. Faraday Trans. I* **77**, 2223 (1981).
- ²¹C. Park, H. M. Kramer, and E. Bauer, *Surf. Sci.* **116**, 467 (1982).
- ²²V. Maurice, J. Oudar, and M. Huber, *Surf. Sci. Lett.* **219**, L628 (1989).
- ²³D. R. Mullins and S. H. Overbury, *Surf. Sci.* **210**, 501 (1989).
- ²⁴Y. Jugnet, N. S. Prakash, L. Porte, T. M. Duc, T. T. A. Nguyen, R. Cinti, H. C. Poon, and G. Grenet, *Phys. Rev. B* **37**, 8066 (1988).
- ²⁵B. Kim, J. Chen, J. L. Erskine, W. N. Mei, and C. M. Wei, *Phys. Rev. B* **48**, 4735 (1993).